Paper:

Underwater Platform for Intelligent Robotics and its Application in Two Visual Tracking Systems

Yuya Nishida*, Takashi Sonoda*, Shinsuke Yasukawa, Kazunori Nagano**, Mamoru Minami***, Kazuo Ishii*, and Tamaki Ura***

*Kyushu Institute of Technology
2-4 Hibikino, Kitakyushu-shi, Fukuoka 808-0196, Japan
E-mail: {ynishida@lsse, t-sonoda@brain, ishii@brain}.kyutech.ac.jp, ura@iis.u-tokyo.ac.jp
**Institute of Industrial Science, The University of Tokyo
4-6-1 Komaba, Meguro-ku, Tokyo 153-8505, Japan
E-mail: yasukawa@liquidinc.asia, k-nagano@iis.u-tokyo.ac.jp
***Graduate School of Natural Science and Technology, Okayama University
3-1 Tsushimanaka, Kita-ku, Okayama-shi, Okayama 700-8530, Japan
E-mail: minami-m@cc.okayama-u.ac.jp
[Received October 3, 2017; accepted March 7, 2018]

A hovering-type autonomous underwater vehicle (AUV) capable of cruising at low altitudes and observing the seafloor using only mounted sensors and payloads was developed for sea-creature survey. The AUV has a local area network (LAN) interface for an additional payload that can acquire navigation data from the AUV and transmit the target value to the AUV. In the handling process of the state flow of an AUV, additional payloads can control the AUV position using the transmitted target value without checking the AUV condition. In the handling process of the state flow of an AUV, additional payloads can control the AUV position using the transmitted target value without checking the AUV condition. In this research, water tank tests and sea trials were performed using an AUV equipped with a visual tracking system developed in other laboratories. The experimental results proved that additional payload can control the AUV position with a standard deviation of 0.1 m.

Keywords: autonomous underwater vehicle, visual tracking, sea-creature sampling

1. Introduction

The seabed contains extremely rich resources such as hydrothermal ore deposits, methane hydrate, and cobalt-rich crust. However, unlike the methods to extract mines and oil fields, no profitable method to extract these resources has been established. One of the reasons for this is that the seabed topographical structure and surrounding environment are mostly unclarified. To conduct a seabed survey at a depth of 50 m or more, to which ordinary divers cannot dive, remotely operated vehicles (ROV) and autonomous underwater vehicles (AUV) are used. An

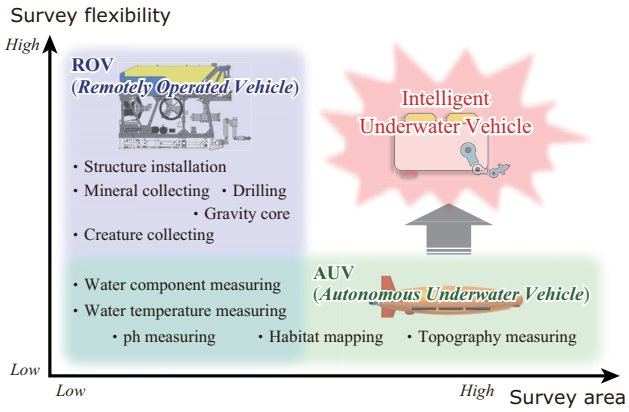

Fig. 1. Tasks performed by underwater vehicles.

ROV receives electric power through umbilical cables and is remotely controlled by a ship whereas all the underwater operations of AUV are programmed prior to its diving into the ocean. **Fig. 1** shows the surveys and tasks conducted with ROV and AUV. The ROV, with a manipulator, is used for surveys and performing operations such as collection of mineral and living sea-creatures [1, 2] as well as core samples [3], drilling into a hydrothermal vent [4], and temperature measurement of water from the vent [5], as it can be operated in accordance with the underwater environment in a flexible manner. An AUV with no constraints due to cables is used for wide area surveys such as measurement of seabed topography and image mapping of biological community [6–8]; however, it cannot perform tasks that require interaction with the surrounding environment. Therefore, ROV and AUV are both necessary, and hence a large operational cost is required to perform a detailed seabed survey that includes wide area mapping of an observation target area and collection of the target during a single navigation. To realize an efficient seabed survey, the authors have been studying an

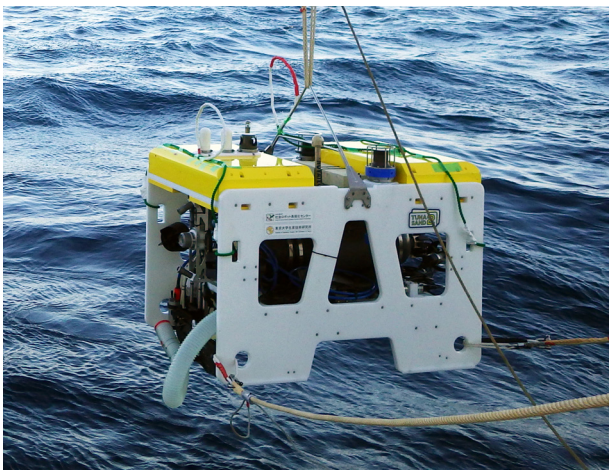

Fig. 2. Hovering type AUV Tuna-Sand2.

AUV that could not only perform a wide area mapping of the seabed, but also undertake sampling or other interactive tasks with the environment. For an AUV to collect an object from a deep ocean seabed in unknown environment and securely return to the sea surface, it needs to have a superior performance and robust software configuration. In this study, as the first step toward the realization of AUV's automatic sampling, we developed an AUV that can control vessel motion according to the designated speed and position while ensuring its safety on the seabed. In this work, the system configuration and kinematics of the developed hovering-type AUV Tuna-Sand2 are introduced, and a sequence of safe surveys and software configuration are proposed. We also report the results of a sampling experiment conducted using a payload developed by Ishii and coworkers of Kyushu Institute of Technology; this experiment verified the effectiveness of the AUV, and a docking experiment was also conducted using a payload developed by Minami and coworkers of Okayama University.

2. Hovering-Type AUV Tuna-Sand2

2.1. System Architecture of the AUV

In this study, we developed AUV Tuna-Sand2 [9] shown in **Fig. 2** on the basis of the technical knowledge of the hovering-type AUV Tuna-Sand [10, 11], obtained from The University of Tokyo. Tuna-Sand2 has two pressure-resistant containers, namely, a control hull and a mapping hull as shown in **Fig. 3**. The payloads for necessary sensors and observation equipment are connected through underwater connectors.

The control hull of the AUV contains three CPUs, one each for navigation, obstacle detection, and 3D mapping, connected with one another through LAN. Various sensors and payloads are connected to the CPU for navigation, which controls all the information and navigation details of the AUV. The latitude and altitude data from the GPS are used for self-localization on the sea surface while the ground speed and altitude data from the Doppler velocity logs (DVL), depth data from pressure sensor, and data of true azimuth and posture from inertial navigation system (INS) are used for underwater self-localization. The CPU for navigation controls the thrusters and tracks a route based on the estimated position and waypoints introduced in advance. An acoustic modem for command link with a function of bidirectional communication is used to receive commands from support ships and transmit AUV navigation information.

A camera, which captures forward images from the AUV, is connected to the CPU for obstacle detection. A sheet laser emits light in forward direction and the camera captures images of the reflected light to detect any obstacle. If an obstacle lies in front of the AUV, the distance to the obstacle is calculated by the light-section method, and the results are transmitted to the CPU for navigation through Ethernet. The observation equipment mounted on the Tuna-Sand2 is a 3D mapping system [12, 13] developed by the Thornton Laboratory of The University of Tokyo. This 3D mapping system consists of a pressure-resistant container, which contains a CPU, control circuit, and two LED strobes. The CPU for mapping controls the lighting interval of the LED strobes and the sheet laser; it also controls the camera to regularly capture laser reflection images and seabed images. The shape of the seabed can be estimated from the acquired laser reflection images, and the color of the seabed can be ascertained from the seabed images. With these data, 3D seabed mosaic images can be created offline. The interface is gigabit Ethernet, through which navigation data can be received and target values are transmitted to control the position of the AUV. The software configurations for payloads are explained in Section 2.4.

2.2. Kinematics

The hovering-type AUV Tuna-Sand2 has six 500 W thrusters, of which four are for horizontal navigation and two for vertical navigation. The location and normal thrust direction of each thruster are presented in **Fig. 4**. To control motions in the surge, sway, and yaw directions and make the maximum forward thrust and the maximum backward thrust the same and the maximum starboard thrust and the maximum port thrust the same, the four horizontal thrusters T_{HFR}, T_{HFL}, T_{HRR}, and T_{HRL} are tilted from the X axis by $-\theta_H$, θ_H, $\pi+\theta_H$, and $\pi-\theta_H$, respectively and placed on the X-Y plane. For efficient placement of the payloads and to prevent the field of vision of the camera from being blocked by the sand dust brought up by current, the two vertical thrusters, T_{VR} and T_{VL}, are placed on the YZ-plane, and tilted from the Z-axis by $-\theta_V$ and θ_V, respectively. For static stability in the roll and pitch directions, the payloads and buoyance materials are placed in such a way that the center of gravity and center of buoyancy both lie on the Z axis and the center of gravity lies below the center of buoyancy. With the thrusts from the thrusters shown in **Fig. 4**, the thrust forces, F_{SRG}, F_{SWY}, and F_{HV} acting on the AUV in the surge, sway, and

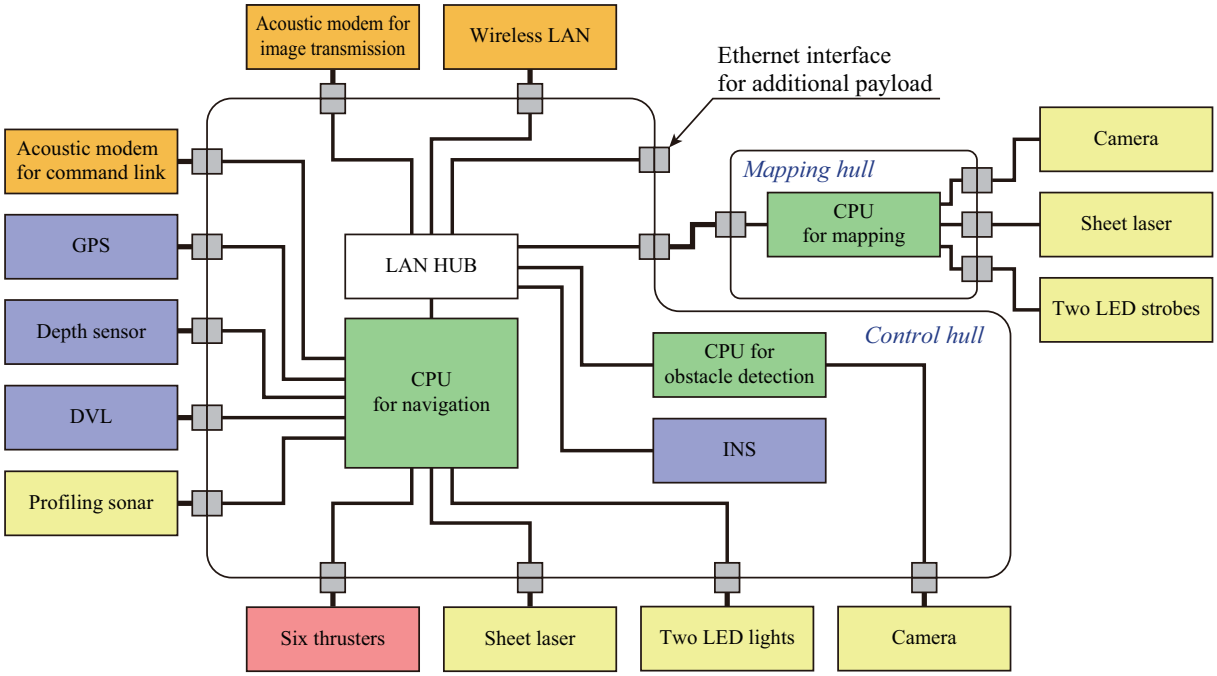

Fig. 3. Block diagram of the AUV Tuna-Sand2.

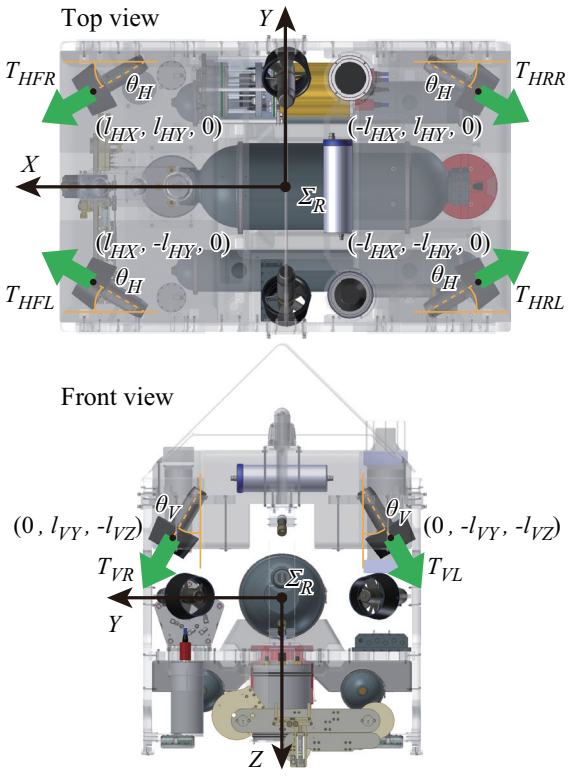

Fig. 4. Location and direction of six thrusters.

heave directions, respectively, and the moments M_{RLL} and M_{YW} in the roll and yaw directions, respectively, are expressed by the following equations. θ_H and θ_V need to be between 0° and $\pi/2$.

$$F_{SRG} = (-T_{HRF} - T_{HFL} + T_{HRR} + T_{HRL})\cos\theta_H \quad (1)$$

$$F_{SWY} = (F_{VR} - F_{VL})\sin\theta_V + (-T_{HFR} + T_{HFL} - T_{HRR} + T_{HRL})\sin\theta_H \quad (2)$$

$$F_{HV} = (F_{VR} - F_{VL})\cos\theta_V \quad (3)$$

$$M_{RLL} = (T_{VR} - T_{VL})(l_{VY}\cos\theta_V + l_{VX}\sin\theta_V) \quad (4)$$

$$M_{YW} = (-T_{HFR} + T_{HFL} + T_{HRR} - T_{HRL}) \cdot (l_{HY}\cos\theta_H + l_{HX}\sin\theta_H) \quad (5)$$

Tuna-Sand2 is not controlled in the roll direction since the restoring moment generated by the gravity and buoyancy is larger than M_{RLL} given by Eq. (4). In this case, the T_{VR} and T_{VL} are determined by F_{HV} as follows.

$$T_{VR} = T_{VL} = \frac{F_{HV}}{2\cos\theta_V} \quad (6)$$

The thrusts of the horizontal thrusters are determined from Eqs. (1), (2), and (5). Here we consider the thrust of the horizontal thrusters necessary to generate F_{SRG}. Since $F_{SWY} = M_{YW} = 0$, for the thrust of the horizontal thrusters to contribute only to F_{SRG}, constraint conditions $T_{HFR} = T_{HFL}$ and $T_{HRR} = T_{HRL}$ have to be satisfied. Because the thrust ratio of the front and rear thrusters $(T_{HFR} + T_{HFL})/(T_{HRR} + T_{HRL})$ is not determined uniquely from Eqs. (1), (2), and (5), we assume the ratio to be 1. From the above constraint conditions, the assumption, and Eq. (1), the following equation is derived.

$$-T_{HFR} = -T_{HFL} = T_{HRR} = T_{HRL} = \frac{F_{SRG}}{4\cos\theta_H} \quad (7)$$

Similarly, the thrust from the horizontal thrusters required to generate F_{SWY} and M_{YW} is calculated and added

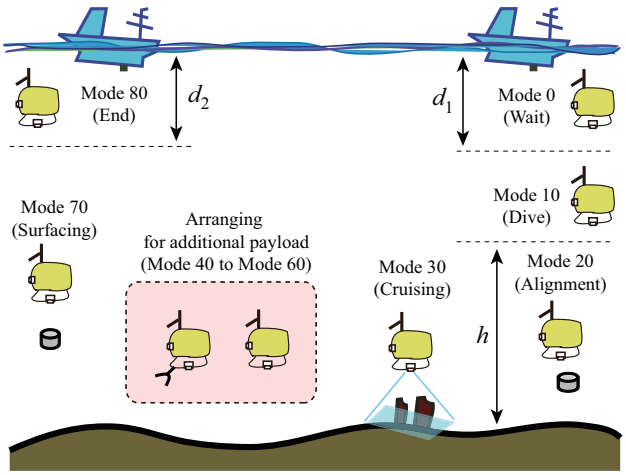

Fig. 5. State flow of the AUV Tuna-Sand2.

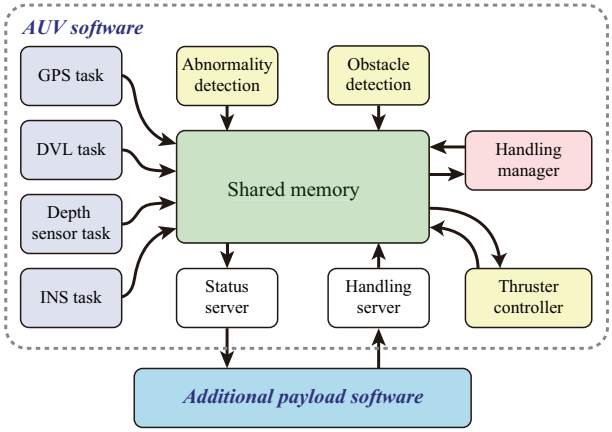

Fig. 6. Software architecture for AUV handling.

to Eq. (7) to obtain the following:

$$T_{HFR} = -aF_{SRG} - bF_{SWY} - cM_{YW} \quad . . . . . (8)$$

$$T_{HFL} = -aF_{SRG} + bF_{SWY} + cM_{YW} \quad . . . . . (9)$$

$$T_{HRR} = aF_{SRG} - bF_{SWY} + cM_{YW} \quad . . . . . (10)$$

$$T_{HRL} = aF_{SRG} + bF_{SWY} - cM_{YW} \quad . . . . . (11)$$

Here, we have

$$a = (4\cos\theta_H)^{-1} \quad . . . . . (12)$$

$$b = (4\sin\theta_H)^{-1} \quad . . . . . (13)$$

$$c = \{4(l_{HY}\cos\theta_H + l_{HX}\sin\theta_H)\}^{-1} \quad . . . . . (14)$$

With the above equations, the arbitrary strengths of F_{SRG}, F_{SWY}, F_{HV}, and M_{YW} can be supplied to the AUV. For the proposed AUV, we assume that F_{SRG}, F_{SWY}, F_{HV}, and M_{YW} are independent variables and are calculated by the PID control of the position or speed.

2.3. State Flow

The operation of Tuna-Sand2 is controlled by a state flow, which is divided into modes and each CPU executes a process according to the mode. The state flow of Tuna-Sand2 is shown in **Fig. 5**. After executing a mission program, the AUV changes its mode to Mode 0 to be ready to dive into the sea. Underwater, the AUV dives with its weight and changes its mode to Mode 10 on reaching depth d_1. In Mode 10, DVL and other sensors as well as the sheet laser whose operation is restricted on ground, are switched on and the altitude is monitored while the AUV keeps diving. When the altitude becomes lower than h, the AUV shifts to Mode 20 and begins controlling the altitude and fixing its position. After hovering at the position for a certain period of time, the AUV changes the mode to Mode 30. In Mode 30, the AUV begins navigation with a constant speed and constant altitude following the predefined waypoints and the CPU for obstruction detection and CPU for mapping execute respective processes. When it passes by all of the waypoints, the AUV changes the mode to next mode. Mode 40 to Mode 60 are reserved for payloads. Using appropriate payloads and mode configuration, the AUV can collect living sea-creatures or perform docking of a seabed station. If there is no payload mode or the payload process finishes, the AUV shifts to Mode 70 and begins surfacing. When it surfaces to depth d_2 or lesser, the AUV judges that it has reached the sea surface; it switches off the DVL and payloads and finishes the session program (Mode 80). The flow from Mode 0 to Mode 80 of the AUV is managed by a mission manager, which executes the processes sequentially.

2.4. Handling System

The CPU for navigation in Tuna-Sand2 manages mode switching and target position in Mode 0 until Mode 30 and in Mode 70 to Mode 80 in the state flow explained in Section 2.3, and executes the processes. On the other hand, Mode 40 to Mode 60 are assigned to the processes for payloads, where the AUV is operated for a target object detection by the external sensors, for example, for collecting seabed sea-creatures and performing docking of a seabed station. **Fig. 6** shows the software configuration of a handling system of Tuna-Sand2. The CPUs for payloads or purposes other than navigation, receive the sensor data stored in a shared memory, navigation information such as PID control, and distance to an obstacle obtained from an obstacle detection task through the status server. Target values and other information in Mode 40 to Mode 60 are stored to the shared memory through a handling server. An abnormality detection task checks for any water leakage in the pressure-resistant vessels and abnormal battery voltage and forces the AUV to surface immediately if any abnormality is present. A handling manager manages the modes and executes the sequence shown in **Fig. 7** for safe navigation of the AUV according to the target values received through the handling server. In Mode 40, the state of the AUV, including the power of necessary equipment such as thrusters and DVL, and the state of communication with the payloads are monitored. If any abnormality is found, the handling process is immediately finished,

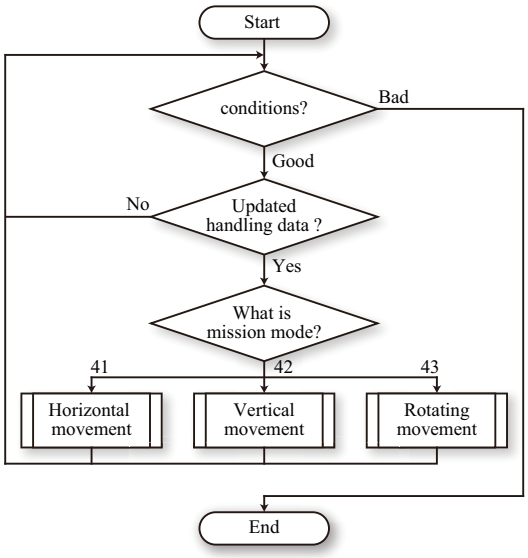

Fig. 7. Flowchart of handling manager.

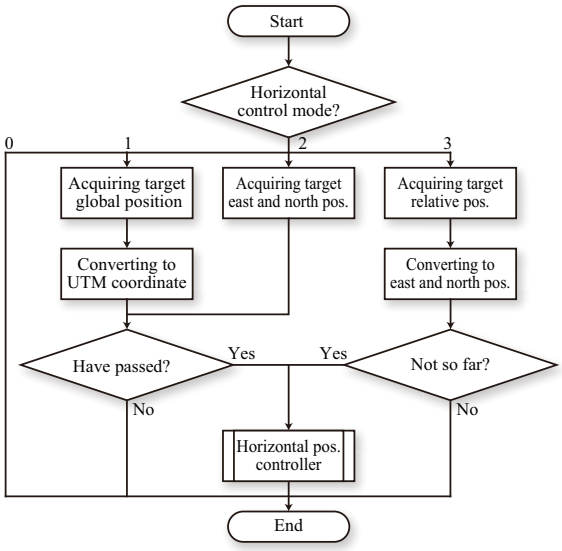

Fig. 8. Flowchart of horizontal movement.

and the mode is changed to Mode 70. If no abnormality is found and the handling data are updated, the current mode is reconfirmed, and actions are taken according to the mode. The horizontal movement is initiated according to the flowchart shown in **Fig. 8**. The payload can instruct target horizontal position in absolute, UTM, or the relative coordinate system by using the horizontal control modes (0 to 3). If the horizontal position is designated with the altitude, latitude, and UTM coordinate system, it is checked whether the AUV passes by the designated position in Mode 30 to ensure the safety. The designation of a target value in the robot coordinate system is limited by the maximum movement distance. All target values can be expressed as those in the UTM coordinate system for horizontal position control, which allows navigation without any erroneous operation.

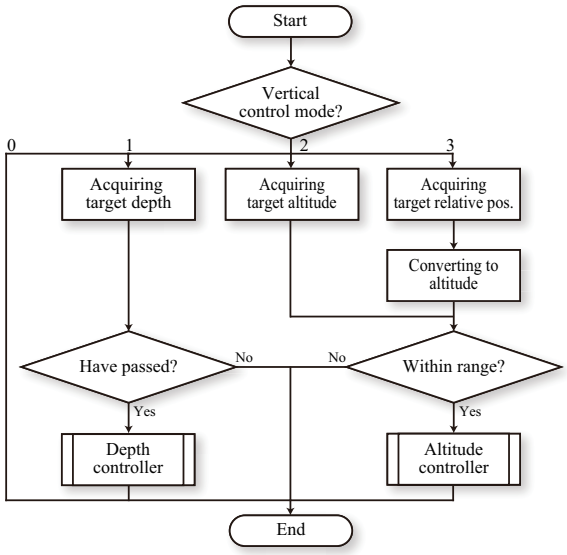

Fig. 9. Flowchart of vertical movement.

The flowchart of the vertical movement is shown in **Fig. 9**. The vertical movement can be designated by using one of the three kinds of target values, namely the depth, altitude, or the heave-direction position in the robot coordinate system. When the depth is designated, it is checked whether the AUV has passed the global positions for horizontal movement as designated. When the AUV navigates with the designation of the altitude or heave-direction position, the DVL may not be able to measure the altitude depending on the distance from the seabed. If the altitude cannot be measured, the altitude cannot be controlled. To prevent this case, it is checked whether the designated position (the altitude converted from the current altitude when the heave-direction position is designated) is within the DVL's measurable range. If not, the control based on the target value is not executed. Because the depth and altitude are measured with respective sensors having different resolutions and sampling intervals, the optimal gain is hardly obtained if the same control system is used to operate the sensors. Because the depth and altitude are measured with respective sensors having different resolutions and sampling intervals, the optimal gain is obtained with difficulty if the same control system is used to operate the sensors. Therefore, the sensors are separately operated using the respective control systems for the vertical movement. The rotation movement can be specified with either of the two target values, specifically, the relative and absolute angles, depending on the control mode. No matter which target value is used, the position is controlled with the absolute angle. Unlike the horizontal or vertical movement, no specific limit is set for the target values of the rotation movement.

Using the above-mentioned handling system, we conducted AUV experiments in a water tank and in an actual sea with the payloads developed by Ishii's group of Kyushu Institute of Technology and by Minami's group of Okayama University.

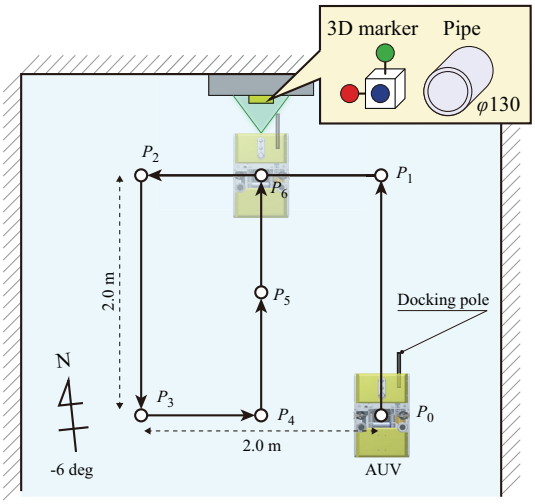

Fig. 10. Setup for docking to station.

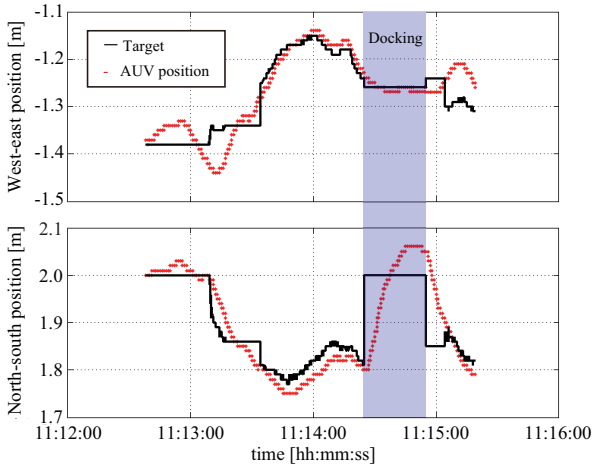

Fig. 11. Position during visual tracking by 3D-MoS.

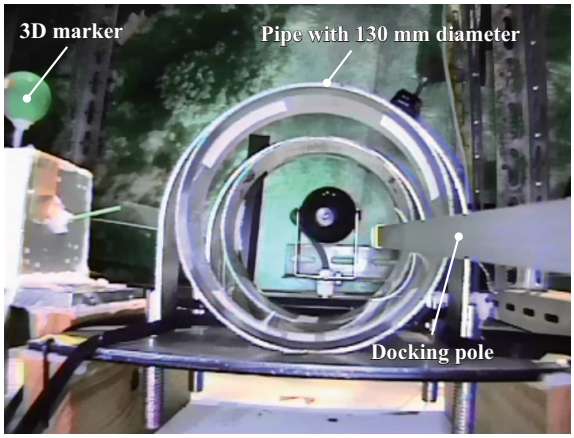

Fig. 12. Captured image by 3D-MoS at docking.

3. Application to Visual Tracking System

3.1. Docking to the Station in a Water Tank

With the payload of a stereo vision system, the "Three-Dimensional Move on Sensing (3D-MoS)" developed by Minami and coworkers of Okayama University, Tuna-Sand2 was used to perform an experiment in which it docked to a station in a water tank. The 3D-MoS, made by Minami's group, uses stereo vision to create a 3D model of a 3D marker having three colored balls, and maps the model to each camera image. The position and posture of the 3D marker at which correlation between the mapped model and the actual images of the 3D marker is maximized are calculated by a genetic algorithm. The relative distance to the target can be measured in real time [14, 15]. **Fig. 10** shows a schematic of the experimental setup. For the experiment, we installed the 3D marker, which 3D-MoS tracked, and a station to a wall of dimensions 8 m × 8 m and 8 m deep pool. The station has a pipe, to which a pole attached to Tuna-Sand2 can be inserted. The 3D marker has three colored balls and the stereo vision system 3D-MoS calculates the marker's position online using a genetic algorithm online and employs the highest-adaptation position as the marker's position. The diameter of the pipe to which the pole is inserted is φ130 mm and the distance from the 3D marker to the pipe is known. In this experiment, the AUV begins navigation in Mode 30 and moves to the waypoints P_0 to P_5 at a depth of 4 m. After reaching P_5, the AUV surfaces to the depth of 1.7 m where the 3D marker is placed, and moves to P_6, at which point, 3D-MoS can recognize the 3D marker. After reaching P_6, the AUV begins visual tracking of 3D-MoS (in Mode 40). When the relative position error between the AUV and 3D marker becomes smaller than a threshold, the AUV performs the docking operation and finishes navigation. In the experiment, the target values given by 3D-MoS are the position data in the robot coordinate system. **Fig. 11** shows the north-south and east-west positions of the AUV in the visual tracking by 3D-MoS. In the experiment, the AUV was designated to move according to the target values from 3D-MoS not only for the horizontal position but also for the depth and direction. However, those data are omitted here, because when it reached P_6, the AUV's relative position errors in the heave and yaw directions converged below the threshold. Although there was an overshoot of approximately 0.05 m in places where the target position changed significantly, Tuna-Sand2 could follow the target values given by 3D-MoS and its position could be controlled within a final error of $\pm$0.01 m or smaller. When the relative position to the target became smaller than the threshold, the AUV immediately moved to the station and successfully performed the docking at the station as shown in **Fig. 12**. Successful insertion of the pole to a φ130 mm pipe indicates that Tuna-Sand2 with 3D-MoS mounted indicates that the relative position to the 3D marker was controlled with the RMS of 0.13 m or smaller, and docking to an actual station was feasible.

3.2. Sampling Test at the Ocean

With a sampling system developed by Ishii and coworkers of Kyushu Institute of Technology, Tuna-Sand2 performed an experiment in which it collected sea-

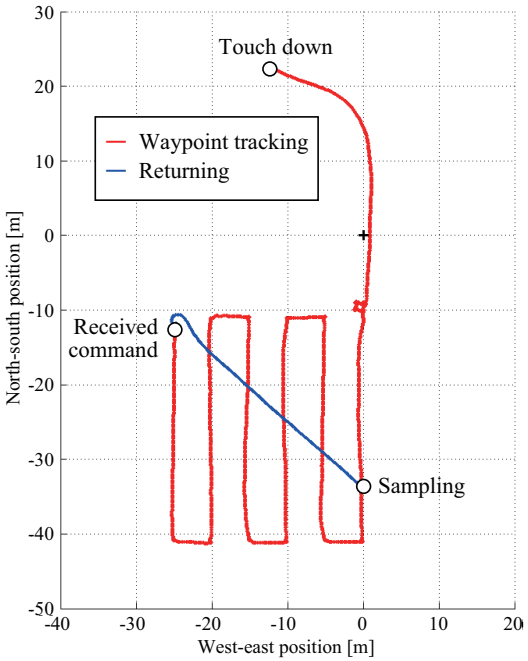

Fig. 13. Trajectory of the AUV in TS2-43 dive.

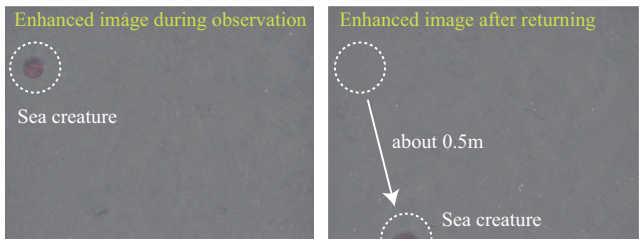

Fig. 14. Comparison of images during observation and return.

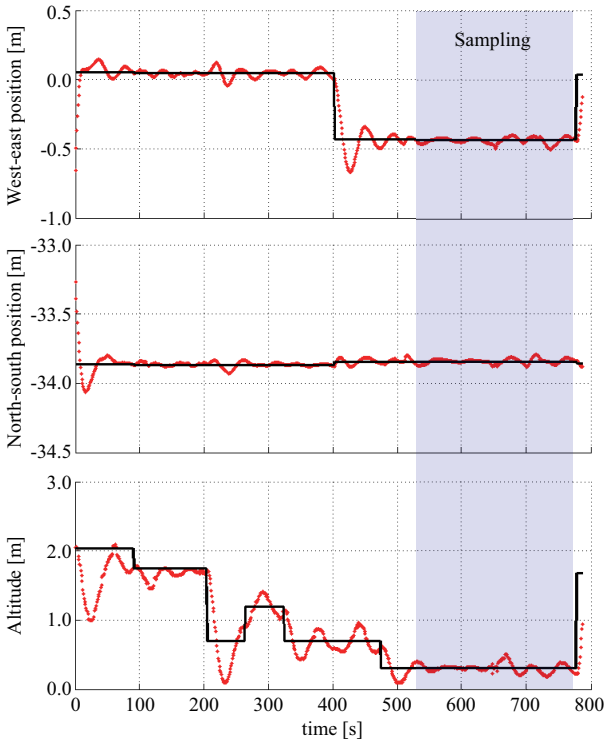

Fig. 15. Position of AUV during visual tracking by sampling system.

creatures at a depth of 450–700 m offshore Hatsushima, Shizuoka Prefecture (KS-17-J03 Research Cruise). The sampling system, made by Ishii's group, consists of a lower-side camera, a manipulator with slurp gun [16–18], and a control container. The sampling system removes lighting irregularity from the captured seabed images [18] and uses a visual attention model [19] to find the highest-attention image as living sea-creatures. The shooting position of the selected image is obtained from the status server and the compressed image is transmitted to the control ship through an image-transmission acoustic modem on Tuna-Sand2 [20]. Researchers on the ship choose a sampling target from the received images and transmit the image number of the image containing the target to the AUV, which then changes the mode to Mode 40. After shifting to Mode 40, the AUV operates under the control of the sampling system and returns to the position where the image of the designated image number was taken. When the AUV reaches the shooting point, the sampling system begins tracking the detected sea-creatures (in Mode 50). When the relative error with the target becomes smaller than the threshold value or when it performs tracking for a designated time, the manipulator with slurp gun performs sampling of the target (in Mode 60).

We conducted a seabed image survey and sampling experiment with Tuna-Sand2 in the sea area offshore Hatsushima. **Fig. 13** shows a trajectory of the AUV in TS-43 dive. After reaching the seabed, the AUV controlled and maintained the altitude at 2.0 m and began navigation to the waypoints with a speed of 0.12 m/s. In approximately 40 min after the start of the navigation, the image number of the image containing a sampling target was designated and the AUV headed to the position where the image was taken. For the AUV navigation, the horizontal movement was controlled by designation of the positions in the north-south and east-west directions in the UTM coordinate system, the vertical movement was controlled by designation of the altitude, and the rotation operation was controlled by designation of the direction toward the image shooting position. **Fig. 14** shows an image captured during the observation (in Mode 30) and another captured when the AUV judged that it had returned to the point where the former image was captured (in Mode 40). The AUV considers that the two images in **Fig. 14** were captured at the same position and therefore the precision of the AUV's position can be determined by comparing the two images. If we assume that the detected sea-creature in the left image of **Fig. 14** did not move until the time when the right image of **Fig. 14** was taken, we can conclude that the AUV can perform self-localization with a precision of ± 0.5 m or smaller. **Fig. 15** shows the position of

AUV while tracking after it returned to the shooting position. The figure indicates that the AUV controlled the horizontal position with the steady-state error of ± 0.1 m or smaller. The vertical movement under the altitude control had larger tremors than the horizontal movement, with an overshoot of as large as 1.0 m. In the experiment, the sampling failed because of wrong recognition of the sampling target. However, the experiment showed that the AUV could successfully accomplish the position control with high precision in the actual sea under the direction from the payload.

4. Conclusions

This paper explains the configuration of a hovering-type AUV, which can navigate with the only the installed sensors and the handling system, which receives operation commands from the payloads. The AUV uses a LAN interface for the payloads, a status server that can acquire the navigation information of the AUV, and a handling server that transmits target values from the payloads to the AUV. The survey of the AUV was conducted sequentially by following a state flow, and the payloads worked in coordination with the AUV by executing processes according to the mode value received from the status server. The modes that can be arranged for the payloads are available in the state flow. In these modes, the payloads can safely control the AUV's position without checking the state of the AUV.

To verify the effectiveness of the AUV and handling system, a payload developed by Ishii and coworkers of Kyushu Institute of Technology and one developed by Minami and coworkers of Okayama University was installed, and experiments with each of the payloads were conducted. The experimental results showed that the AUV and handling system worked correctly both in the water tank and at sea, and the position of the AUV could be controlled with a precision of ± 0.1 m by using the payloads.

Acknowledgements

This work was supported by the Japan Science and Technology CREST grant program for the "Establishment of core technology for the preservation and regeneration of marine biodiversity and ecosystems," Grant Number JPMJCR11A2. The authors would like to thank the research vessel Shinsei-maru crew and Japan Agency for Marine-Earth Science and Technology (JAMSTEC) during the KS-17-J03 research cruise.

References:

[1] C. E. Fitzgerald and K. M. Gillis, "Hydrothermal Manganese Oxide Deposits from Baby Bare Seamount in the Northeast Pacific Ocean," Marine Geology, Vol.225, Issues 1-4, pp. 145-156, 2006.

[2] S. Thatje, S. Hall, C. Hauton, C. Held, and P. Tyler, "Encounter of Lithodid Crab Paralomis Birsteini on the Continental Slope off Antarctica," Sampled by ROV, Polar Biology, Vol.31, Issue 9, pp. 1143-1148, 2008.

[3] H. Yoshida, S. Ishibashi, Y. Watanabe, T. Inoue, J. Tahara, T. Sawa, and H. Osawa, "The ABISMO Mud and Water Sampling ROV for Surveys at 11,000 m Depth," Marine Technology Society J., Vol.43, No.5, pp. 87-96, 2009.

[4] S. Kawagucci, J. Miyazaki, R. Nakajima, T. Nozaki, Y. Takaya, Y. Kato, T. Shibuya, U. Konno, Y. Nakaguchi, K. Hatada, H. Hiroyama, K. Fujikura, Y. Furushima, H. Yamamoto, T. Watsuji, J. Ishibashi, and K. Takai, "Post-drilling Changes in Fluid Discharge Pattern, Mineral Deposition, and Fluid Chemistry in the Iheya North Hydrothermal Field, Okinawa Trough," Geochemistry, Geophysics, Geosystems, Vol.14, Issue 11, pp. 4774-4790, 2013.

[5] J. Hashimoto, S. Ohta, T. Gamo, H. Chiba, T. Yamaguchi, S. Tsuchida, T. Okudaira, H. Watabe, T. Yamanaka, and M. Kitazawa, "First Hydrothermal Vent Communities from the Indian Ocean Discovered," Zoological Science, Vol.18, No.5, pp. 717-721, 2001.

[6] M. Grasmueck, G. P. Eberli, D. A. Viggiano, T. Correa, G. Rathwell, and J. Luo, "Autonomous underwater vehicle (AUV) mapping reveals coral mound distribution, morphology, and oceanography in deep water of the Straits of Florida," Geophysical Research Letters, Vol.33, Issue 23, L23616, 2006.

[7] M. Johnson-Roverson, O. Pizarro, S. B. Williams, and I. Mahon, "Generation and visualization of large-scale three-dimensional reconstructions from underwater robotics surveys," J. of Field Robotics, Vol.27, Issue 1, pp. 21-51, 2009.

[8] B. Thorton, A. Bodenmann, O. Pizarro, S. B. Williams, A. Friedman, R. Nakajima, K. Takai, K. Motoki, T. Watsuji, H. Hirayama, Y. Matsui, H. Watanabe, and T. Ura, "Biometric assessment of deep-sea vent megabenthic communities using multi-resolution 3D image reconstructions," Deep Sea Research Part I: Oceanographic Research Papers, Vol.116, pp. 200-219, 2016.

[9] Y. Nishida, T. Sonoda, S. Yasukawa, J. Ahn, K. Nagano, K. Ishii, and T. Ura, "Development of an autonomous underwater vehicle with human-aware robot navigation," Procs. of IEEE/OTS OCEANS, 16506112, Monterey, 2016.

[10] Y. Nishida, T. Ura, T. Nakatani, T. Sakamaki, J. Kojima, Y. Itoh, and K. Kim, "Autonomous Underwater Vehicle "Tuna-Sand" for Image Observation of the Seafloor at a Low Altitude," J. of Robotics and Mechatronics, Vol.26, No.4, pp. 519-521, 2014.

[11] Y. Nishida, T. Ura, T. Hamatsu, K. Nagahashi, S. Inaba, and T. Nakatani, "Resource Investigation for Kichiji Rockfish by Autonomous Underwater Vehicle in Kitami-Yamato Bank off Northern Japan," ROBOMECH J., Vol.1, No.2, pp. 1-6, 2014.

[12] A. Bodenmann, B. Thornton, and T. Ura, "3D Mapping of the Seafloor in Color Using a Single Camera: Benthicmapping Based on Video Recordings and Laser Profiling to Generate Colored 3D Reconstructions of the Seafloor," Sea Technol., Vol.51, No.12, pp. 51-53, 2012.

[13] B. Thornton, A. Asada, A.Bodenmann, M. Sagekar, and T. Ura, "Instruments and Methods for Acoustic and Visual Survey of Manganese Crusts," J. of Oceanic Engineering, Vol.38, No.1, pp. 186-203, 2013.

[14] W. Song, F. Yu, and M. Minami, "3D visual servoing by feedforward evolutionary recognition," J. of Advanced Mechanical Design, Systems, and Manufacturing, Vol.4, No.4, pp. 739-755, 2010.

[15] F. Yu, M. Minami, W. Song, and A. Yanou, "Eye-vergence visual servoing enhancing Lyapunov-stable trackability," Artificial Life and Robotics, Vol.18, No.1-2, pp. 27-35, 2013.

[16] T. Sonoda, A. A. F. Nassiraei, I. Godler, T. Weerakoon, and K. Ishii, "Development of Hydraulic Underwater Manipulator for Deep-sea Survey AUV," Procs. of ICRAOB, pp. 242-245, 2017.

[17] T. Weerakoon, T. Sonoda, A. A. F. Nassiraei, I. Godler, and K. Ishii, "Underwater Manipulator for Sampling Mission with AUV in Dee-Sea," Procs. of JSME Conf. on Robotics and Mechatronics, 2P1-F11, 2017.

[18] A. Jonghyun, S. Yasukawa, T. Sonoda, T. Ura, and K. Ishii, "Erratum to: Enhancement of Deep-sea Floor Image Obtained by an Underwater Vehicle and Its Evaluation by Crab Recognition," J. of Marine Science and Technology, Vol.22, No.4, pp. 758-770, 2017.

[19] L. Itti and C. Koch, "A saliency-based search mechanism for overt and covert shifts of visual attention," Vision research, Vol.40, No.10, pp. 1489-1506.

[20] A. Jonghyun, S. Yasukawa, T. Sonoda, Y. Nishida, K. Kazuo, and T. Ura, "Image Enhancement and Compression of Deep-sea Floor Image for Acoustic Transmission," Proc. of MTS/IEEE OCEANS, CFP16OCF-ART, 2016.

Name:
Yuya Nishida

Affiliation:
Project Assistant Professor, Frontier Research Academy for Young Researchers, Kyushu Institute of Technology

Address:
2-4 Hibikino, Wakamatsu-ku, Kitakyushu, Tokyo 808-0196, Japan

Brief Biographical History:
2011- Researcher, Kyushu Institute of Technology
2012- Project Researcher, Institute of Industrial Science, The University of Tokyo
2015- Project Assistant Professor, Kyushu Institute of Technology

Main Works:
• "Design Principle of High Power Joint Mechanism Possible to Walking and Jumping Imitating Locust Leg Structure," J. of Robotics and Mechatronics, Vol.23, No.2, pp. 225-230, 2011.
• "Resource Investigation for Kichiji Rockfish by Autonomous Underwater Vehicle in Kitami-Yamato Bank off Northern Japan," ROBOMECH J., Vol.1, Issue 1:2, pp. 1-6, 2014.

Membership in Academic Societies:
• The Japan Society of Mechanical Engineers (JSME)
• The Robotics Society of Japan (RSJ)
• The Japanese Society of Fisheries Science

Name:
Takashi Sonoda

Affiliation:
Kyushu Institute of Technology

Address:
2-4 Hibikino, Wakamatsu-ku, Kitakyushu 808-0196, Japan

Brief Biographical History:
2009- Researcher, Fukuoka Industry, Science and Technology Foundation
2012- Researcher, Kyushu Institute of Technology
2015- Research Associate Professor, Kyushu Institute of Technology

Main Works:
• "Development of antagonistic wire-driven joint employing kinematic transmission mechanism," J. of Automation, Mobile Robotics & Intelligent Systems, Vol.4, No.2, pp. 62-70, 2010.
• "Modeling and Evaluation of a Twist Drive Actuator for Soft Robotics," Advanced Robotics, Vol.26, No.7, pp. 765-783, 2012.

Membership in Academic Societies:
• The Robotics Society of Japan (RSJ)
• The Society of Instrument and Control Engineers (SICE)

Name:
Shinsuke Yasukawa

Affiliation:
The University of Tokyo
Recreation Lab, Inc.

Address:
4-6-1 Komaba, Meguro-ku, Tokyo 153-8505, Japan
4F Otemachi Bldg., 1-6-1 Otemachi, Chiyoda-ku, Tokyo 100-0004, Japan

Brief Biographical History:
2014-2017 Research Associate, Kyushu Institute of Technology
2017 Received Ph.D., Division of Electrical, Electronic and Information Engineering, Osaka University
2017- Researcher, Recreation Lab, Inc.
2017- Research Associate, The University of Tokyo

Main Works:
• "A Vision Sensor System with a Real-Time Multi-Scale Filtering Function," Int. J. of Mechatronics and Automation, Vol.4, No.4, pp. 248-258, 2014.
• "Real-Time Object Tracking Based on Scale-Invariant Features Employing Bio-Inspired Hardware," Neural Networks, Vol.81, pp. 29-38, 2016.

Membership in Academic Societies:
• The Robotics Society of Japan (RSJ)
• The Society of Instrument and Control Engineers (SICE)

Name:
Kazunori Nagano

Affiliation:
Project Researcher, Institute of Industrial Science, The University of Tokyo

Address:
4-6-1 Komaba, Meguro-ku, Tokyo 153-8505, Japan

Brief Biographical History:
2013- Joined Mitsui Engineering and Shipbuilding Co., Ltd.
2014- Project Researcher, Institute of Industrial Science, The University of Tokyo

Name:
Mamoru Minami

Affiliation:
Professor, Graduate School of Natural Science and Technology, Okayama University

Address:
3-1-1 Tsushimanaka, Okayama 700-8530, Japan

Brief Biographical History:
1994- Associate Professor, Department of Mechanical Engineering, University of Fukui
2002- Professor, Department of Human and Artificial Intelligence Systems, University of Fukui
2010- Professor, Graduate School of Natural Science and Technology, Okayama University

Main Works:
• "Dual-eyes Vision-based Docking System for Autonomous Underwater Vehicle: An Approach and Experiments," J. of Intelligent & Robotic Systems, Doi: 10.1007/s10846-017-0703-6, 2017.
• "Visual Servoing to catch fish Using Global/local GA Search," IEEE/ASME Trans. on Mechatronics, Vol.10, No.3, pp. 352-357, 2005.
• "Reconfiguration Manipulability Analyses for Redundant Robots," Trans. of the ASME, J. of Mechanisms and Robotics, Vol.5, No.4, pp. 1-16, 2013.

Membership in Academic Societies:
• The Institute of Electrical and Electronics Engineers (IEEE)
• The Japan Society of Mechanical Engineers (JSME)
• The Society of Instrument and Control Engineers (SICE)
• The Robotics Society of Japan (RSJ)

Name:
Kazuo Ishii

Affiliation:
Professor, Department of Human Intelligence Systems, Kyushu Institute of Technology

Address:
2-4 Hibikino, Wakamatsu-ku, Kitakyushu, Fukuoka 808-0196, Japan

Brief Biographical History:
1996- Researcher, Institute of Industrial Science, The University of Tokyo
1996-1998 Assistant Professor, Kyushu Institute of Technology
1998-2011 Associate Professor, Kyushu Institute of Technology
2011- Professor, Kyushu Institute of Technology

Main Works:
• "Enhancement of deep-sea floor images obtained by an underwater vehicle and its evaluation by crab recognition," J. of Marine Science and Technology, Vol.22, Issue 4, pp. 758-770, 2017.

Membership in Academic Societies:
• The Institute of Electrical and Electronics Engineers (IEEE)
• The Japan Society of Mechanical Engineers (JSME)
• The Robotics Society of Japan (RSJ)
• The Institute of Electrical and Electronics Engineers (IEEE)

Name:
Tamaki Ura

Affiliation:
Center for Socio-Robotic Synthesis, Kyushu Institute of Technology

Address:
2-4 Hibikino, Wakamatsu-ku, Kitakyushu, Fukuoka 808-0196, Japan

Brief Biographical History:
1992-2013 Professor, The University of Tokyo
2013- Professor, Kyushu Institute of Technology

Main Works:
• Development and operation of AUV "r2D4"

Membership in Academic Societies:
• The Institute of Electrical and Electronics Engineers (IEEE) Oceanic Engineering Society (OES), Fellow
• The Robotics Society of Japan (RSJ)
• The Japan Society of Naval Architects and Ocean Engineers